11-1-2011

Removal of 2,4-dichlorophenoxyacetic Acid by Calcined Zn–Al–Zr Layered Double Hydroxide

Allen Chaparadza
Marquette University

Jeanne Hossenlopp
Marquette University, jeanne.hossenlopp@marquette.edu

Accepted version. *Journal of Colloid and Interface Science*, Vol. 363, No 1 (November 2011): 92-97. DOI.

Removal of 2,4-dichlorophenoxyacetic acid by calcined Zn–Al–Zr layered double hydroxide

Allen Chaparadza
Department of Chemistry, Marquette University
Milwaukee, WI

Jeanne M. Hossenlopp
Department of Chemistry, Marquette University
Milwaukee, WI

Abstract:

The adsorption equilibrium, kinetics, and thermodynamics of removal of 2,4-dichlorophenoxy-acetic acid (2,4-D) from aqueous solutions by a calcined Zn–Al layered double hydroxide incorporated with Zr^{4+} were studied with respect to time, temperature, pH, and initial 2,4-D concentration. Zr^{4+} incorporation into the LDH was used to enhance 2,4-D uptake by creating higher positive charges and surface/layer modification of the adsorbent. The LDH was capable of removing up to 98% of 2,4-D from 5 to 400 ppm aqueous at adsorbent dosages of 500 and 5000 mg L^{-1}. The adsorption was described by a Langmuir-type isotherm. The percentage 2,4-D removed was directly proportional to the adsorbent dosage and was optimized with 8% Zr^{4+} ion content, relative to the total metals (Zr^{4+} + Al^{3+} + Zn^{2+}). Selected mass transfer and kinetic models were applied to the experimental data to examine

Journal of Colloid and Interface Science, Vol. 363, No. 1 (August 2011): pg. 92-97. DOI.

uptake mechanism. The boundary layer and intra-particle diffusion played important roles in the adsorption mechanisms of 2,4-D, and the kinetics followed a pseudo-second order kinetic model with an enthalpy, ΔH_{ads} of -27.7 ± 0.9 kJ mol^{-1}. Regeneration studies showed a 6% reduction in 2,4-D uptake capacity over six adsorption–desorption cycles when exposed to an analyte concentration of 100 ppm.

Keywords: sol-gel synthesis, layered double hydroxides, adsorption, 2,4-dichlorophenoxyacetic acid, Langmuir isotherm.

1. Introduction

The herbicide 2,4-dichlorophenoxy acetic acid (2,4-D), a well known endocrine disruptor [1], is still commonly used because of its low cost and good selectivity. Applications include control of broad leaf weeds in cereal crops, pastures and in gardens [2]. Extensive use and poor biodegradability of 2,4-D has resulted in its ubiquitous presence in the environment and has led to contamination of surface and ground waters [3]. It is considered moderately toxic and the maximum allowable concentration in drinking water is 30 ppb [4]. Methods for removal of 2,4-D from water and soils include photo catalytic degradation, physical–chemical and biological methods. The use of layered double layered hydroxides (LDHs) as alternative materials for the removal of 2,4-D from water has been explored [2], [5], [6], [7], [8], [9] and [10].

LDHs are a group of inorganic layered materials consisting of brucite-like layers. They can be represented by the general formula: $[M^{2+}_{1-x}M^{3+}_{x}(OH)_2]^{x+}[X^{m-}_{\frac{x}{m}}.nH_2O]$, where M^{2+} and M^{3+} are divalent and trivalent cations that occupy octahedral positions in the brucite-like layer, and X^{m-} is an interlayer anion [5]. LDHs can take up anions from solution by three different mechanisms: interlayer anion exchange, surface adsorption, and reconstruction of the calcined LDH by the "memory effect" [11]. The regeneration capacity of layered double hydroxides after calcinations and its capability to uptake anions through different mechanisms makes them very good candidates for removing anionic pollutants. In this paper we present a study of the adsorption of 2,4-D by Zr^{4+}-incorporated Zn/Al LDH, demonstrating the ability to optimize adsorption capacity by modifying the metal ion composition of the metal hydroxide layer in a ternary LDH.

2. Materials and methods

2.1. LDH synthesis

LDHs with various Zn:Al:Zr atomic ratios and carbonate anions were synthesized by the co-precipitation method [12] at room temperature by reacting aqueous solutions containing a mixture of $Zn(NO_3)_2$, $Al(NO_3)_3{\cdot}9H_2O$ and $ZrCl_4$. A solution containing 0.3 mol L^{-1} Na_2CO_3 and 2 mol L^{-1} NaOH was added slowly to the precursor solutions under vigorous stirring while maintaining the pH between 8 and 8.5. The resulting slurries were stirred at 70 °C for 1 h, filtered and washed with water until filtrate was pH 7, and then dried at 80 °C and then calcined at 280 °C for 1 h before use.

2.2. LDH characterization

Powder X-ray diffraction (PXRD) studies were conducted on a Rigaku Miniflex 2 diffractometer, in the Bragg θ–2θ geometry, equipped with a Cu Kα radiation (λ = 1.5418 Å), operating at a voltage of 30 kV and a current of 15 mA using angular step sizes of 0.083° (2θ) from 2° to 85°. The average crystallite sizes were evaluated using the (0 0 3) reflection with the Debye–Scherrer method [13]. Metals composition analysis was performed using a Perkin Elmer ICP-AES 5300 DV instrument. The carbon and hydrogen analysis were performed at Huffman Labs on a custom built analyzer which uses coulometric detection as described in [14]. The elemental analysis results are shown in Tables S1 and S2 in Supporting information. Ultraviolet–visible (UV–Vis) diffuse reflectance spectra (DRS) of the powders were obtained using a Perkin Elmer Lambda 35 spectrometer (see Fig. S1 in Supporting information).

2.3. Determination of point of zero charge pH (pH_{pzc})

The point of zero charge pH (pH_{pzc}) was determined following the procedure described by Sharma and coworkers [15]. 0.01 mol L^{-1} NaCl was prepared and its pH was adjusted to between 2 and 12 using HCl and NaOH. 50 mL of the approximately 0.01 mol L^{-1} NaCl solutions was mixed with 0.2 g of the ZnAlZr LDH and left for 48 h and then the pH was measured using an Orion 3 Star pH meter. The initial

pH was then plotted against the final pH and the point where this curve intersects the plot of $pH_{initial} = pH_{final}$ is the pH_{pzc}.

The effect of the initial solution pH on the adsorption of 2,4-D was evaluated using an adsorbent dosage of 500 mg L^{-1} and 100 ppm 2,4-D solutions. The pH was initially adjusted with 0.01–1 mol L^{-1} HNO_3 and NH_4OH solutions. The resulting LDH suspensions were left to stand at room temperature for 24 h and the concentrations of 2,4-D remaining in solution were then determined by ultraviolet–visible (UV–Vis) spectroscopy monitoring the 2,4-D absorption peak at 283 nm.

2.4. Sorption experiments

The sorption of 2,4-D was studied by batch-type equilibrium experiments at room temperature. 2,4-D solutions, with concentrations ranging from 100 to 2000 ppm, were prepared by dissolving 2,4-dichlorophenoxyacetic acid in 2% ethanol in water solution. The pH of the solutions varied from 3.2 to 3.69 depending on 2,4-D concentration. Different amounts (70–500 mg) of Zn–Al–Zr–CO_3 were dispersed in 100 mL of the 2,4-D solutions; when the sorbents were added the pH increased to 7–7.5. The flasks were left standing until equilibrium was reached; 8 h was found to be sufficient for this purpose. The suspension was then filtered and the filtrate was analyzed for 2,4-D concentration. The amount of adsorption q was calculated by [10]:

$$q_t = \frac{(C_i - C_t)V}{m} \qquad \text{Equation (1)}$$

where C_i is the initial 2,4-D concentration and C_t is the concentration at time (t) in solution, m is the mass of the sorbent and V is the volume of solution.

2.5. Effect of pH on adsorption

The effect of the starting solution pH on the adsorption of 2,4-D was evaluated using 100 ppm solutions at an adsorbent dosage of 500 mg L^{-1}. The starting solution pH was initially adjusted with 0.01–1 mol L^{-1} HNO_3 and NH_4OH solutions and was determined by an Orion

3 Star pH meter. The resulting LDH suspensions were left standing for 8 h and then residual 2,4-D left in solution was analyzed as above.

2.6. Effect of competing anions

One hundred parts per million of 2,4-D solutions were prepared with 0.005–0.1 mol L^{-1} of competing ions. The competing anions, I^-, Cl^-, ClO_4^- ClO4-, CH_3COO^-, $S_2O_3^{2-}$ S2O32-, $CO_3$2-CO32-, and PO_4^{3-} PO43-, were prepared from their corresponding sodium salts. In the pH range used in this study, the main phosphate ion which competed with 2,4-D was HPO_4^{2-} HPO42- and the carbonate ion was HCO_3^- HCO3-. A LDH adsorbent dose of 500 mg/L was added to each solution and the samples were sealed and left at room temperature for 8 h and then analyzed as above.

2.7. Regeneration/re-use experiments

For regeneration testing, 0.5 g of the LDHs exposed to 500 ppm 2,4-D for 8 h were mixed with 100 ml of 50% ethanol in water solution and agitated for 1 h at 50 °C. The solid sorbents were then filtered and calcined at 280 °C for 2 h. They were then characterized by PXRD and finally subjected to successive adsorption- desorption cycles.

3. Results and discussion

3.1. Characterization of the calcined and uncalcined LDH

Representative PXRD patterns of the Zn:Al:Zr LDH with Zn:Al:Zr atomic ratios ranging from 3:1:0 to 3:0.60:0.40 are shown in Fig. 1. Elemental analysis results are provided as Supporting information. The PXRD patterns of the Zn–Al–Zr–CO_3 showed three equally spaced peaks at 2θ values of 11.5°, 23° and 34.5° consistent with hydrotalcites (JCPDS:41-1428) with a hexagonal crystal structure [16].

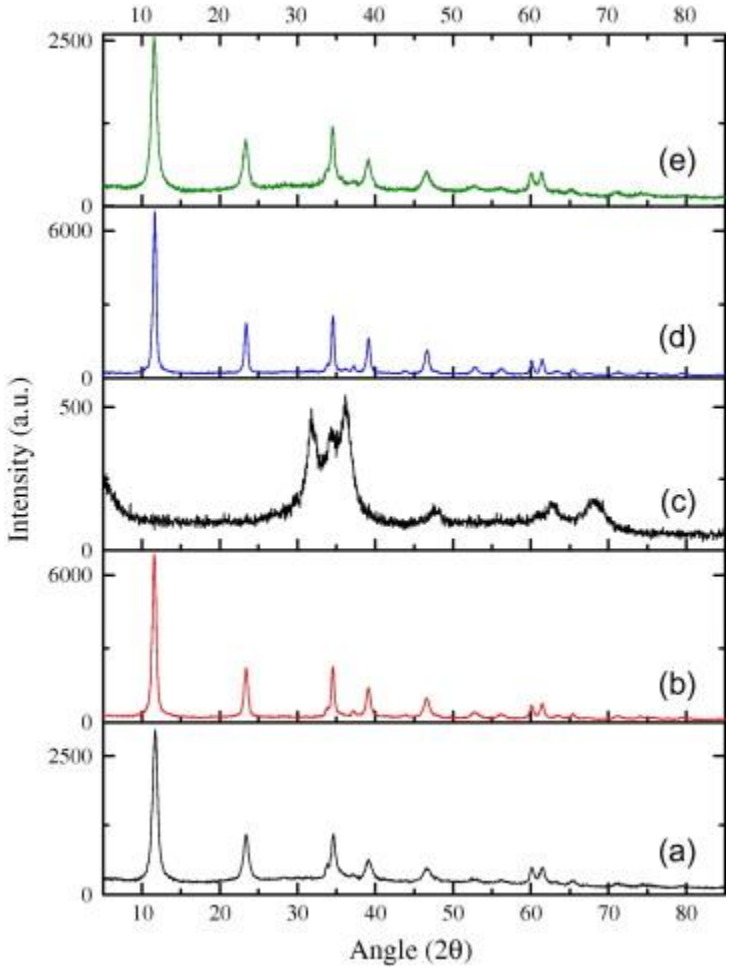

Fig. 1. XRD patterns of the ZnAlZr-LDH samples with different Zn:Al:Zr ratios used during synthesis (a) 3:1:0, (b) 3:0.85:0.15, (c and d) 3:0.67:0.33, (e) 3:0.60:0.40. The mean crystallite sizes were 20.5 ± 1.7, 18 ± 1.2, 13.5 ± 0.9 and 11.2 ± 2.1 nm for (a, b, d and e) respectively. Samples (a, b, d and e) were uncalcined and (c) was calcined at 280 °C. The phase at 280 °C, while not well crystallized, is consistent with ZnO.

The crystallinity and the mean crystallite size, as determined with the Scherrer equation, decreased with increasing the Zr content (see Fig. 1 caption). The decrease in mean crystallite size with increasing Zr content is likely related to the surface charge, with electrostatic forces thus playing a role in controlling crystal growth. A higher Zr content would increase the charge density of the LDH and consequently causing an increase in the magnitude of the zeta potential, the higher the zeta potential the smaller the particle size. Similar effects have been observed on surface nucleation of tin

hydroxides prepared through a sol–gel technique using stannous chloride [17]. This decrease may also be attributed to the formation of amorphous zirconium species on the LDH surface.

The temperature at which the LDH is calcined should be sufficiently high to eliminate most of the carbonate anions and any other anions in the interlayer region and low enough that it does not preclude the structural reconstruction. A temperature of 280 °C was chosen for the calcination temperature based on thermo gravimetric analysis (TGA) and differential scanning calorimetry (DSC) shown in Supporting information (Figs. S2 and S3). TGA shows that the loss of interlayer CO_3^{2-} CO32- takes place at about 275 °C and this is further supported by the exothermic DSC peak between 200 and 275 °C.

By substituting Al^{3+} (0.053 nm) with Zr^{4+} which has a larger ionic radius (0.072 nm), an increase in the lattice *a* parameter is expected. The lattice parameter, *a*, was calculated using $a = 2\ d_{(110)}$ [18] and the values were in the range of 0.3074–0.3079 nm. These values are consistent with Zr-free samples [19], contrary to expectation. However, Tichit and coworkers have also reported the similar findings within the same Zr^{4+} range; Zr^{4+} incorporation into Mg–Al LDHs did not have an observable effect on the lattice, *a* parameter [20]. The invariance of the *a* parameter maybe due to the formation of a separate hydrozincite phase not detectable by PXRD.

UV–Vis DRS was used to evaluate whether there was any significant solid–solid phase separation [19] and results are shown in more detail in Supporting information (Fig. S4). Evidence was obtained for a charge transfer band involving isolated Zr^{4+} species [21] and [22] but not for the characteristic ZrO_2 band at 230 nm [23] and [24]. This is also supported by PXRD results which do not show the existence of a ZrO_2 phase.

3.2. Effect of Zr content on 2,4-D removal

Zr^{4+} has been shown to modify the layer charge and induce higher basicity of mixed oxides as a result of the formation of Zr^{4+}–O^{2-} acid–base pairs [22]. In addition, it has also been shown to improve the adsorption properties of complex carbon mineral adsorbents [25].

Journal of Colloid and Interface Science, Vol. 363, No. 1 (August 2011): pg. 92-97. DOI.

Fig. 2 shows the amount of 2,4-D removed as a function of Zr^{4+} content. LDHs with no Zr exhibited very poor 2,4-D adsorption.

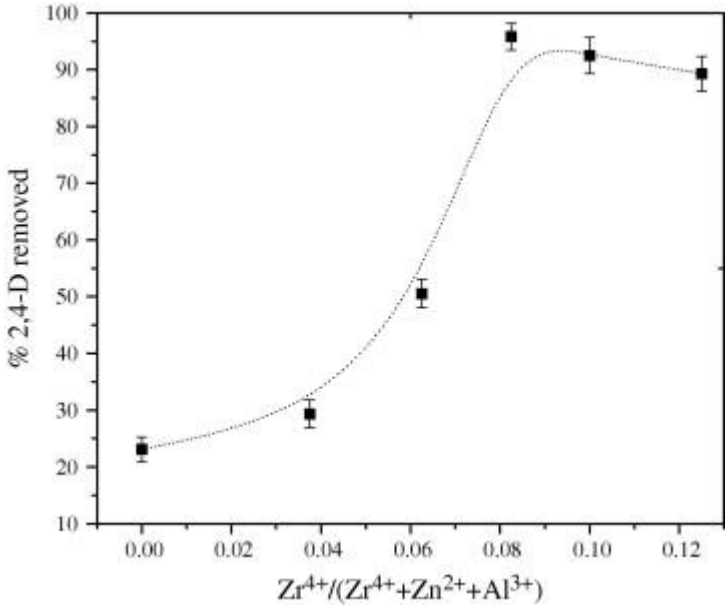

Fig. 2. Percentage 2,4-D removal as a function of Zr^{4+} content used during synthesis. The initial 2,4-D concentration was 300 ppm and the adsorbent dosage was 5000 mg L^{-1}.

The amount adsorbed increased with increasing Zr content up to a $Zr^{4+}/(Zr^{4+} + Zn^{2+} + Al^{3+})$ fraction of 0.083 and then decreased with further increases in Zr content. The mechanism behind the enhancement of adsorption with Zr is not yet well understood. One possibility is that Zr^{4+} ions occupy interstitial sites within the LDHs and, as a result, lower the LDHs surface potential, hence lowering the energy for 2,4-D adsorption. At higher Zr levels, the crystallinity as well as the adsorption capability of the LDHs decreases. This decrease may be attributed to solid–solid phase separation between the Zr and the LDH and as a result other amorphous phases might be beginning to form. This kind of phase separation is not uncommon at the nanoscale level [26]. No change was observed in the PXRD patterns after exposure of the LDHs to solutions containing 2,4-dichlorophenoxyacetic acid (see Fig. S4 in Supporting information). This indicates that adsorption, rather than anion exchange, is the dominant mode of uptake.

An LDH with a Zn:Al:Zr ratio of 3:0.67:0.33 and molecular formula $Zn_{4.4}AlZr_{0.3}(CO_3)_{1.1}(OH)_{10.8}1.7H_2O$ (see Tables S1 and S2 in

Supporting information for the detailed elemental analysis results) and calcined at 280 °C was found to be the best at removing 2,4-D and all studies were performed using this mixed oxide.

3.3. Adsorption kinetics

The adsorption kinetics were investigated to determine the equilibrium time for 2,4-D sorption onto the LDH at room temperature. Experiments were carried out with an initial 2,4-D concentration of 100 mg L^{-1} and different adsorbent dosages which ranged from 0.07 to 5 g L^{-1}. The time required to reach equilibrium was between 1–5 h and was inversely proportional to the adsorbent mass as can be seen in Fig. 3. At higher adsorbent dosage (5000 mg L^{-1}) the uptake is quicker and higher in terms of the amount of 2,4-D removed because of the availability of many adsorption sites. At lower adsorbent dosages, as seen in the case of 70 mg L^{-1}, there are a limited number of sites for the same 2,4-D concentration. As a result the adsorption process is slow and amount of 2,4-D removed from solution is low.

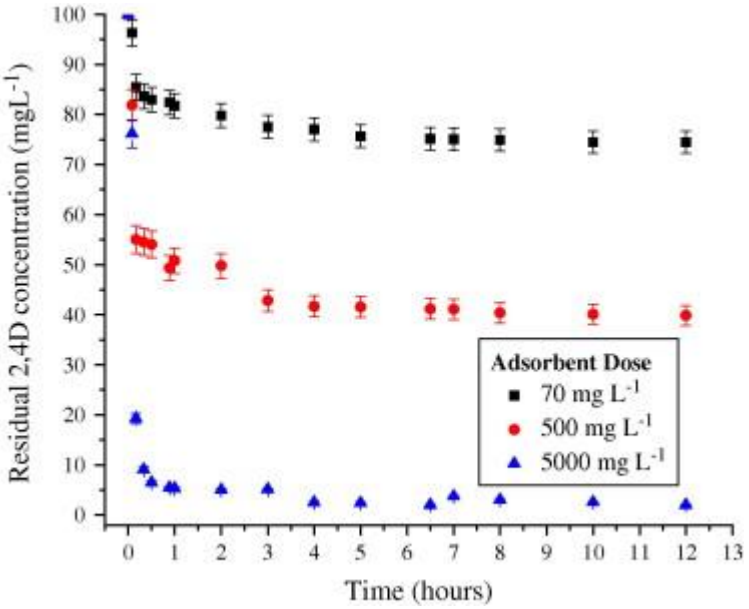

Fig. 3. Amount of 2,4-D left as a function of time at different adsorbent masses.

For sorption that is preceded by diffusion through a boundary, the kinetics likely follows the pseudo-first or pseudo-second order Lagergren equations expressed as Eqs. (2) and (3) respectively [27] and [28].

Journal of Colloid and Interface Science, Vol. 363, No. 1 (August 2011): pg. 92-97. DOI.

$$\log(q_e - q_t) = \log q_e - \left(\frac{k_1}{2.303}\right) t \qquad (2)$$

$$\frac{t}{q_t} = \frac{1}{k_2 q_e^2} + \left(\frac{1}{q_e}\right) t \qquad (3)$$

where q_e and q_t are the amounts of 2,4-D adsorbed at equilibrium in mg/g, and at time t in h, respectively, k_1 and k_2 are the pseudo first-order rate constant (h^{-1}) and second order rate constant (g mg^{-1} h^{-1}) respectively. The pseudo-first and -second order constants and correlation coefficients, are determined from the linear plots of ln ($q_e - q_t$) and t/q_t against time and are shown in Fig. S5 of the Supporting information). The pseudo-first order model did not fit the data as well as the pseudo-second order model as indicated in the results shown in Table 1.

Adsorbent dosage (mg/L)	$q_{e,\ exp}$ (mg/g)	First order kinetic model			Second order kinetic model		
		k_1(1/h)	$q_{e\ mod}$	r^2	k_2(g/mg h)	$q_{e\ mod}$	r^2
70	192.3	0.51	177.8	0.98	0.004	213.2	0.99
500	95.1	0.55	36.8	0.92	0.05	96.4	0.99
5000	28.6	1.39	3.1	0.67	1.6	28.7	0.99

Table 1. Comparison of the pseudo-first and pseudo-second order rate constants and calculated and experimental q_e values obtained at different adsorbent dosages.

From the second order model, increasing the adsorbent mass caused an increase in the sorption rate and this could be due to an increase in the number of available adsorption sites as adsorbent mass is increased.

3.4. Adsorption mechanism

The 2,4-D removal sorption can be described as a four step process involving; (i) transport of the 2,4-D in the bulk solution, (ii)

subsurface region diffusion, (iii) migration of sorbate within the pores of the LDH (intra-particle diffusion), and (iv) binding of the 2,4-D on the active sites [29] and [30]. The slowest of these steps determines the overall rate of the adsorption process. When intra-particle diffusion plays a major role in the adsorption process the rate of diffusion is a function of $t^{1/2}$ and according to Weber and Morris can be defined as follows [31]:

$$q_t = f\left(\frac{Dt}{r_p^2}\right)^{1/2} = k_{id}t^{1/2} \qquad (4)$$

where r_p is particle radius, D is the effective diffusivity of solutes within the particle, k_{id} (mg g^{-1} $h^{1/2}$) is the intra-particle diffusion rate constant.

Fig. 4 shows the plot of amount adsorbed, q_t (mg g^{-1}), versus $t^{1/2}$. The sorption process is not a one-step process as evidenced by the curvature in these plots.

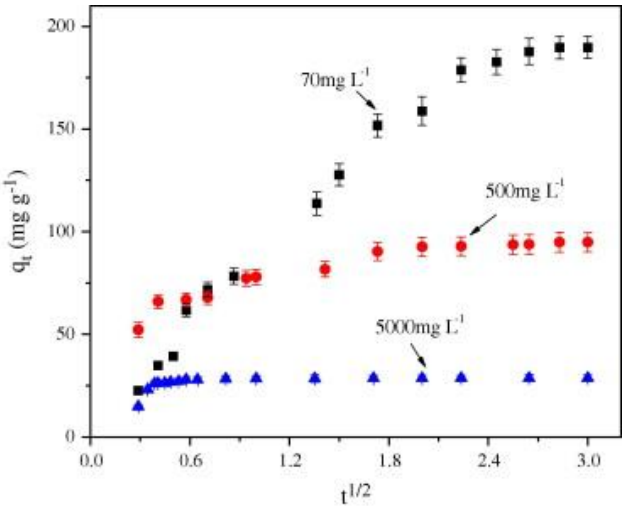

Fig. 4. Intra-particle diffusion plots for 2,4-D adsorption on ZnAlZr LDH at different adsorbent dosages

The initial phase of the adsorption can be attributed to instantaneous external diffusion, whereas the second portion indicates a relatively slower adsorption when the adsorbate diffuses gradually

into the interior surfaces of the particles and the adsorption becomes intra-particle diffusion controlled [32]. When equilibrium is reached, the intra-particle diffusion slows down due to saturation of most of the adsorption sites and this is evidenced by the plateaus.

The slope of the second portion of the plot (Fig. S6 in Supporting information) defines the intra-particle diffusion rate constant and the intercept reflects the boundary layer effect. The results are consistent with intra-particle diffusion not being the sole rate-controlling factor. The adsorption of 2,4-D by the ZnAlZr LDH appears to be a complex process, involving both boundary layer and intra-particle diffusion.

3.5. Adsorption isotherms

The sorption of 2,4-D by the Zn/Al/Zr ternary LDH was evaluated by fitting to Langmuir isotherm of the type [33]:

$$q_e = \frac{q_{max} K C_e}{1 + K C_e} \qquad (5)$$

where q_e is the amount adsorbed at equilibrium in mg g^{-1} and C_e is the concentration at equilibrium, K is the adsorption equilibrium constant (L mol^{-1}) and q_{max} is the maximum amount removed from solution. By plotting q_e versus C_e (Fig. 5), reasonably good fits were obtained indicating the general conformity of the data to the Langmuir isotherm.

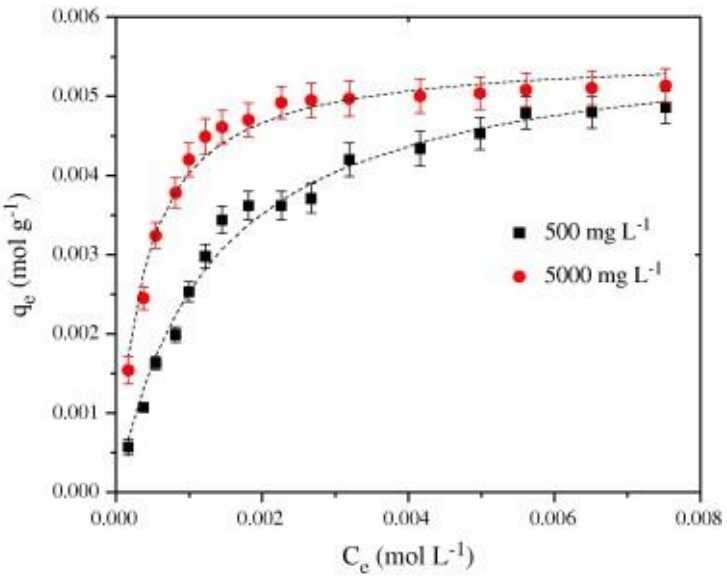

Journal of Colloid and Interface Science, Vol. 363, No. 1 (August 2011): pg. 92-97. DOI.

Fig. 5. Adsorption isotherms of 2,4-D adsorption on ZnAlZr-LDH.

The Langmuir constants K and q_{max}, determined using non-linear least squares analyses, are shown in Table 2.

Adsorbent dosage (mg L^{-1})	q_{max} (mmol g^{-1})	K (L mmol L^{-1})	r^2
500	5.8±0.1	0.8±0.3	0.996
5000	5.9±0.2	2.7±0.2	0.989

Table 2. Langmuir parameters for the adsorption of 2,4-D by different masses of the ZnAlZr LDH in 1 L solution.

Conformity of the 2,4-D adsorption data to the Langmuir model indicates that the sorbate–sorbent interaction was much stronger than the solvent–sorbent interaction at the adsorption sites [34]. The affinity constant, K, changes with the adsorbent mass, 0.8 and 2.7 mmol L^{-1} for 500 mg L^{-1} and 5000 mg L^{-1} adsorbent respectively. This is an indication that the type of interaction between the LDH and the herbicide is not the same when adsorbent mass is changed. However, the maximum amount (q_{max}) adsorbed remains constant. Table 3 compares the adsorption capacity of different adsorbents used for the removal of 2,4-D. From the comparison of the adsorption capacity, q_{max}, the ZnAlZr ternary LDH in this study is larger than those in most previous work.

The heat of adsorption ΔH for the sorption of 2,4-D onto ZnAlZr-LDH can be calculated from the temperature dependence of the equilibrium adsorption constant, K, by the Clausius-Claperyon equation [35]:

$$\frac{\partial log K}{\partial(\frac{1}{T})} = -\frac{-\Delta \mathrm{H}_{ads}}{2.303R} \qquad (6)$$

A plot of log K versus $1/T$ (see insert in Fig. 6), should be linear with slope $-\Delta H_{ads}/2.303R$ and intercept $\Delta S_{ads}/2.303\mathrm{R}$. ΔH_{ads} was found to be -27.7 ± 0.9 kJ mol^{-1} while ΔS_{ads} was -0.047 ± 0.05 kJ $K^{-1}mol^{-1}$ giving a Gibbs free energy of -14.1 ± 0.5 kJ mol^{-1}. The ΔH_{ads} is approximately of the same as those reported for the adsorption of 2,4-

D on other surfaces. Ackay et al. [36] reported a 2,4-D adsorption enthalpy on dodecylammoniumsepiolite of −24.6 kJ mol^{-1} and Sexton and Haque [37] reported −8.4 kJ mol^{-1} on humic acid. The relatively low heat of adsorption suggest that 2,4-D adsorption was a physical, van der Waals or hydrogen bond type [38]. From temperature dependent studies (Fig. 6), the adsorption increased with increasing temperature up to 60 °C and then decreased when temperatures >60 °C. This type of behavior is usually displayed in systems where there is a weak interaction between sorbent and adsorbate.

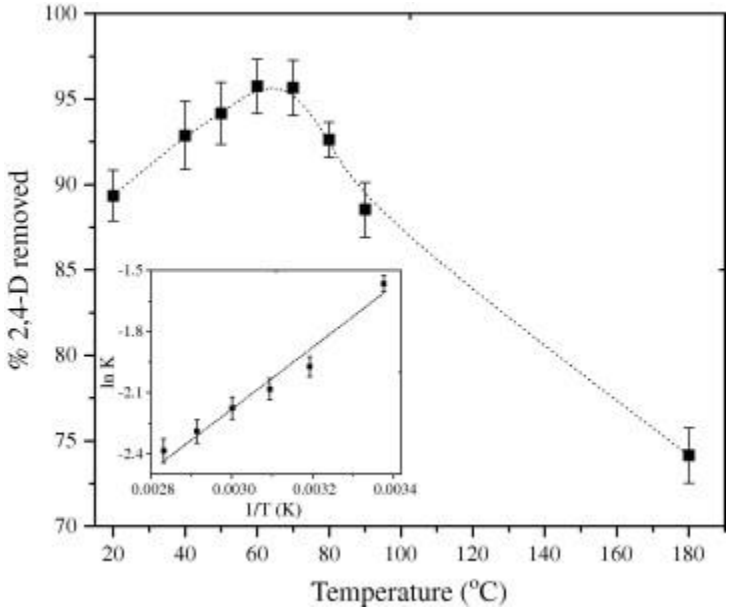

Fig. 6. Temperature dependent adsorption of 2,4-D onto the ZnAlZr-LDH. Insert shows the plot of log *K* vs 1/*T* used to determine the thermodynamic parameters of adsorption. The initial 2,4-D concentration was 100 ppm and the adsorbent dosage was 500 mg L^{-1}.

3.6. Effect of pH and competing anions

The effect of initial pH on the adsorption of 2,4-D, from solutions with an initial concentration of 100 ppm, on the LDHs is shown in Fig. 7. The data indicate that the amount of 2,4-D adsorbed is maximized in the pH range 2–8.5. At pH > 9, the adsorption decreases sharply with increasing pH. The pH at point of zero charge, (pH_{pzc}), which indicates the electrical neutrality of the adsorbent surface at particular pH for the calcined Zn/Al/Zr LDH, was 9.2. The

surface of an LDH is negatively charged when pH > pH_{pzc}[39]. At pH > 9, 2,4-D ionizes to the oxyanion form and as result is repelled from the surface hence the decrease in the amount of 2,4-D adsorbed at pH greater than 9.

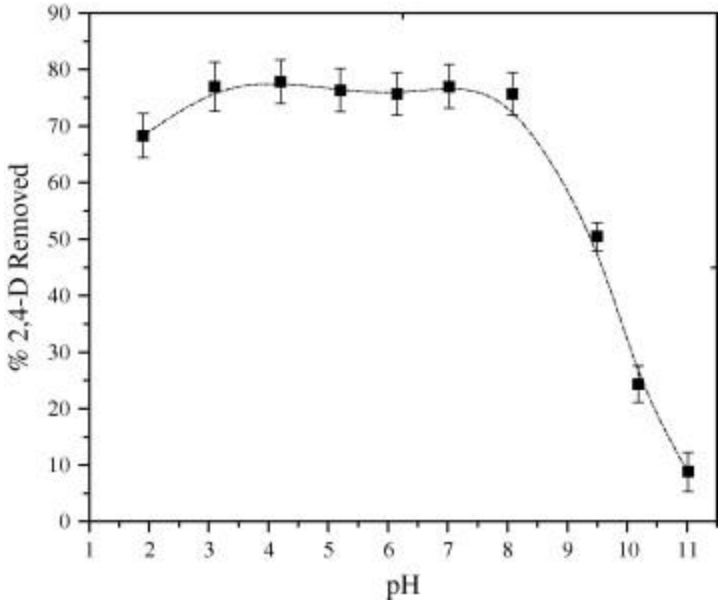

Fig. 7. Effect of pH on 2,4-D removal.

Fig. 8 shows the adsorption of 2,4-D in the presence of competing anions.

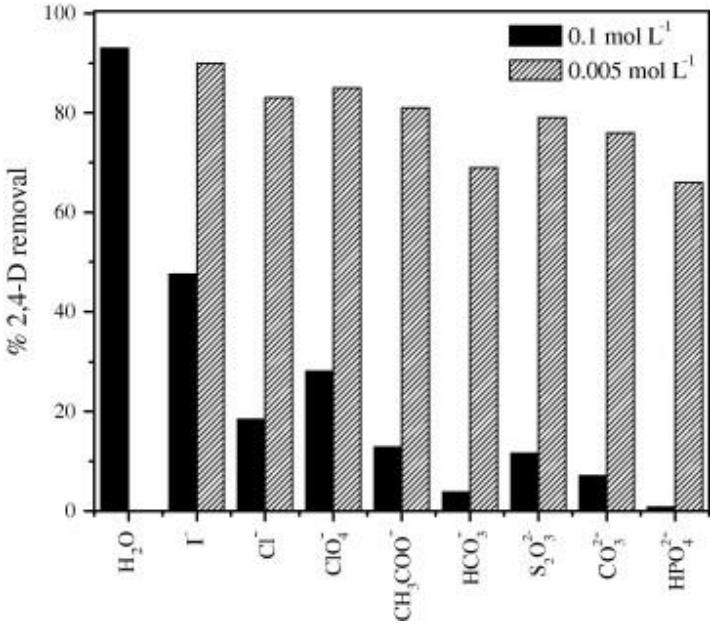

Journal of Colloid and Interface Science, Vol. 363, No. 1 (August 2011): pg. 92-97. DOI.

Fig. 8. Effect of competing anions and concentration on the adsorption of 2,4-D on ZnAlZr-LDH with an initial concentration of 100 ppm and an adsorbent dosage of 5000 mg L^{-1}.

In the absence of competing anions 98% of the herbicide was removed from a 100 ppm solution by an adsorbent dosage of 5000 mg L^{-1}. A higher concentration (0.005–0.1 mol L^{-1}) of ions than what is found in most natural waters [39] is used here in order to clearly observe the trends in competitive uptake. The experimental data indicate that HPO_4^{2-} (introduced as Na_3PO_4) [40] has the greatest effect on adsorption of 2,4-D onto the ZnAlZr LDH. Carbonates were introduced through Na_2CO_3. In this case, CO_3^{2-} and HCO_3^- coexist in the solutions in the concentration range used, so the term carbonates represent both $CO_3^{2-}$and HCO_3^- with the latter being the main ions present in solution [41]. The extent of 2,4-D adsorption decreased in the order: $I^- < ClO_4^- < Cl^- < CH_3COO^- < \frac{HCO_3^-}{CO_3^{2-}} < HPO_4^{2-}$. Generally LDHs have greater affinity for ions with greater charge density [42].

3.7. Desorption and recovery studies

Desorption is an important feature of a material for its repeated use for the removal of contaminants. After 2,4-D exposure, the ZnAlZr LDH was washed with 50% ethanol–water solution to help aid the 2,4-D desorption from the LDH surface and then heated at 280 °C for 4 h in air. At this temperature, 2,4-D is decomposed and thus removed from the adsorbent. When the LDH was heated at 280 °C it temporarily lost its layered structure only to reconstitute after being added to water (see Fig. S4 in Supporting material). The reconstituted LDH was capable of removing 2,4-D to nearly the same extent as the original material. For six cycles of adsorption and desorption starting with an initial 2,4-D concentration of 100 ppm there was a 6% reduction in the amount of 2,4-D removed by the regenerated LDH. When the initial concentration of 2,4-D was increased to 1000 ppm the reduction over six cycles was 25%. These results demonstrate that a higher 2,4-D concentration shortens the effective lifetime of the adsorbent.

4. Conclusions

Calcined ZnAlZr ternary LDH can be used for the removal of 2,4-D from aqueous solutions. The LDH was capable of removing up to 98% of 2,4-D from solutions whose initial concentrations were between 5 and 400 ppm. The percentage removed was directly proportional to the amount of adsorbent but decreased in the presence of competing ions. The adsorption is spontaneous as indicated by ΔH_{ads} which is -27.7 kJ mol^{-1} and follows pseudo-second order kinetics. The adsorption mechanism can be summarized as complex with some intra-particle diffusion and the adsorption is described by the Langmuir type isotherm. Recovery through thermal decomposition lowers the probability of the pollutant finding its way back into water systems.

Acknowledgment

This work was supported by the National Science Foundation (CHE-0809751).

Supporting Information

Elemental analyses, PXRD and UV-vis characterization of LDHs, details for psuedo-first order kinetics, and intraparticale diffusion data are provided in Supporting Information.

References

1. T. Colborn, F. S. Vom Saal, A. M. Soto, *Env.Imp.Ass.Rev.***14**(1993), pp 469-489.

2. A. Mantilla, F. Tzompantzi, J.L. Fernández, J.A.I. Díaz Góngora, G. Mendoza and R. Gómez, *Catal. Today* **148**(2009), pp 119-123.

3. J. C. Pichat, J. F. D'Oliveria, D. Mas, J. F. Maffre, in *Photocatalytic Purification and Treatment of Water and Air*, H. Al-Ekabi and D. F. Ollis, Eds.,(Elsevier, Amsterdam, (1993).

4. World Health Organization, Guidelines for drinking-water quality, World Health Organisation, Geneva, ed. 3rd, (2004), pp. 191-196.

5. L. P. Cardoso and J. B. Valim, *J. Phys. Chem. Solids* **67**(2005), pp 987-993.

6. Y. F. Chao, P. C. Chen, S. L. Wang, *Appl. Clay Sci.* **40**(2008), pp 193-200.

7. Y. F. Chao, J. J. Lee, S. L. Wang, *J. Hazard. Mater.* **165**(2009), pp 846-852.

8. M. C. Hermosin and J. Cornejo, *Chemos.* **24**(1992), pp 1493-1503.

9. S. U. Khan, *Environ. Sci. Technol.* **8**(1974), pp 236-238.

10. A. Legrouri, M. Lakraimi, A. Barroug, A. De Roy, J. P. Besse, *Water Res.* **39**(2005), pp 3441-3448.

11. R. C. T. Slade and D. G. Evans, Layered double hydroxides: Structure and Bonding Springer-Verlag, Berlin, (2006), pp. 1-87.

12. J. S. Valente, F. Tzompantzi, J. Prince, J. G. H. Cortez, R. Gomez, *Appl. Catal.,*B**90**(2009), pp 330-338.

13. P. Scherrer, *Nachr.Ges.Wiss.Göttingen*(1918) pp 98-100.

14. E. W. D. Huffman, *Microchem. J.* **22**(1977), pp 567-573.

15. Y. C. Sharma, V. Srivasta, C. H. Weng, S. N. Upadhayay, *Can. J. Chem. Eng.* **87**(2009), pp 921-929.

16. A. S. Bookin, V. I. Cherkashin, V. A. Drits, *Clays Clay Min.* **41** (1993), pp 558-564.

17. A. Chaparadza, S. B. Rananavare, V. Shutthanandan, *Mater. Chem. Phys.* **102**(2007), pp 176-180.

18. V. Rives and S. Kannan, *J. Mater. Chem.* **10**(2000), pp 489-495.

19. F. Kooli, C. Depege, A. Ennaqadi, A. De Roy, J. P. Besse, *Clay Clay Min.***45**(1997), pp 92-98.

20. D. Tichit, N. Das, B. Coq, R. Durand, *Chem. Mater.* **14**(2002), pp 1530-1538.

21. B. Rakshe, V. Ramaswamy, A. V. Ramaswamy, *J. Catal.* **163**(1996), pp 501-505.

22. A. Tuel, S. Gontier, R. Teissier, *Chem.Commun.*(1996), pp 651-652.

23. D. Ciuparu, A. Ensuque, G. Shafeev, F. Bozon-Verduraz, *J. Mater. Sci. Lett.* **19**(2000), pp 931-933.

24. S. Velu, V. Ramaswamy, S. Sivasanker, *Chem. Commun.*(1997), pp 2107-2108.

25. R. Leboda, A. Gierak, Z. Hubicki, A. Lodyga, *Mater. Chem. Phys.* **30**(1991), pp 83-91.

26. A. Chaparadza and S. B. Rananavare, *Nanotech.* **21**(2010), p 035708.

27. S. Lagergren, *Kung. Sven. Veten.Handlin.***24**(1898), 1-39.

28. H. Yuh-Shan, *Scientom.* **59**(2004), pp 171-177.

29. W. Plazinski and W. Rudzinski, *J. Phys. Chem. C***113**(2009), pp 12495-12501.

30. J. J. Pignatello and B. Xing, *Environ. Sci. Technol.* **30**(1995), pp 1-11.

31. W. J. Weber and J. C. Morris, *J.Sanit.Eng.Div.ASCE* **89**(1963), p 31.

32. F. C. Wu, R. L. Tseng, R. S. Juang, *J. Hazard. Mat.* **73** (2000), pp 63-75.

33. Z. Aksu and E. Kabasakal, *Sep. Purif. Technol.* **35**(2004), pp 223-240.

34. L. El Gaini, E. Sebbar, Y. Boughaleb, M. Bakasse, M. Lakraimi, A. Meghea, *Nonlin. Optics Quan. Optics* **38** (2008), pp 191-203.

35. H. Baker and F. Khalili, *Anal. Chim. Acta* **516**(2004), pp 179-186.

36. G. Akcay, M. Akcay, K. Yurdakoc, *J. Colloid Interface Sci.* **281**(2005), 27-32.

37. R. Haque and R. Sexton, *J. Colloid Interface Sci .***27**(1968), 818-827.

38. S. Glasstone and D. Lewis, Element of Physical Chemistry (D. Van Nostrand Company Inc., New Jersey, 1962), pp. 558-570.

39. L. Yang, Z. Shahrivari, P. K. T. Liu, M. Sahimi, T. T. Tsotsis, *Ind. Eng. Chem. Res.* **44** (2005), 6804-6815.

40. K. Karageorgiou, M.Paschalis, G. N. Anastassakis, *J. Hazard. Mat.* **139** (2007), pp 447-452

41. H. Greenway, W. Armstrong, T. D. Colmer, *Annals of Botany* **98** (2006), 9–32.

42. S. Miyata, *Clays Clay Min.* **31**(1983), 305-311.

About the Authors

Jeanne M. Hossenlopp : Department of Chemistry, Marquette University, PO Box 1881, Milwaukee, WI 53201-1881, United States

Fax: +1 414 288 7066.

Email: jeanne.hossenlopp@marquette.edu

Supporting Information For:

Removal of 2,4-Dichlorophenoxy acetic acid by calcined Zn/Al/Zr Layered Double Hydroxides

*Allen Chaparadza and Jeanne M. Hossenlopp**

Department of Chemistry
Marquette University
PO Box 1881
Milwaukee, WI 53201-1881

7 pages, 6 figures and 5 tables

*Corresponding author: email: jeanne.hossenlopp@marquette.edu, tel: 414-288-3537, fax: 414-288-7066

Journal of Colloid and Interface Science, Vol. 363, No. 1 (August 2011): pg. 92-97. DOI.

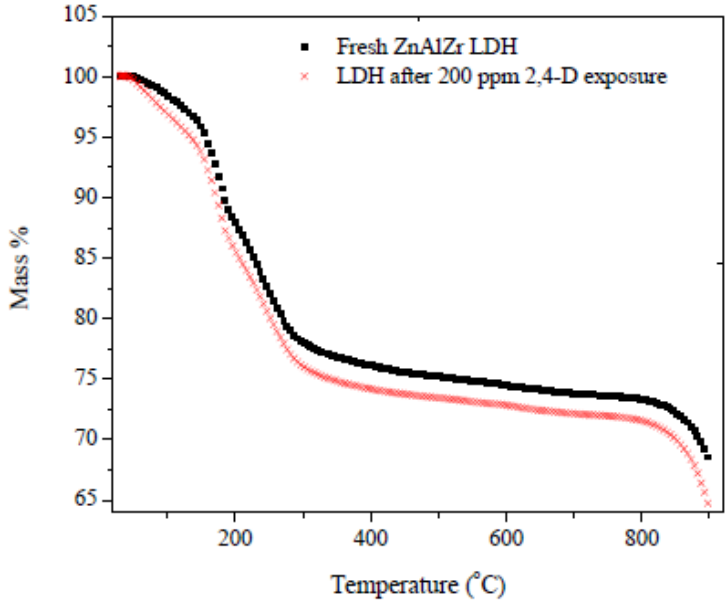

Figure S1. Thermogravimetric analysis of the fresh and 2,4-D exposed ZnAlZr LDH

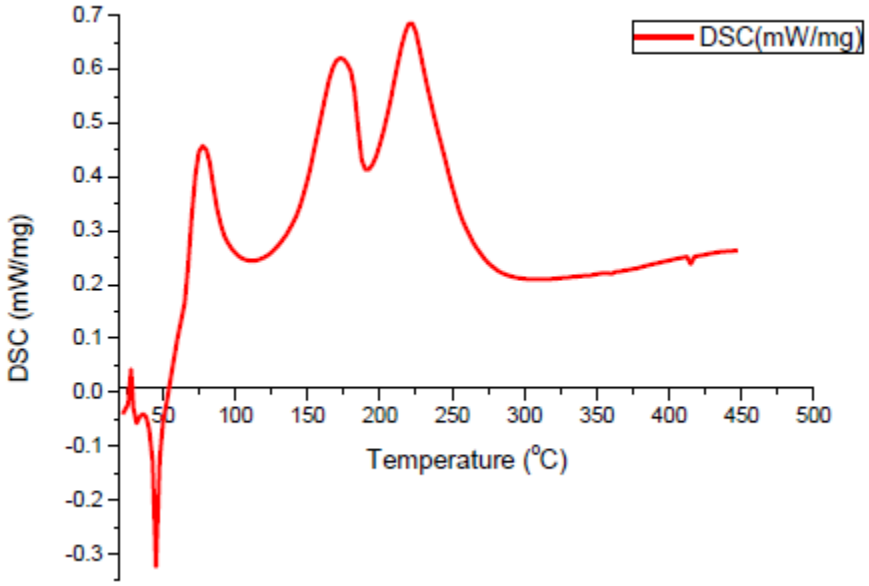

Figure S2. DSC results for the ZnAlZr-LDH sample with Zn:Al:Zr ratio of 3:0.67:0.33 after it had been exposed to 200 ppm 2,4-D.

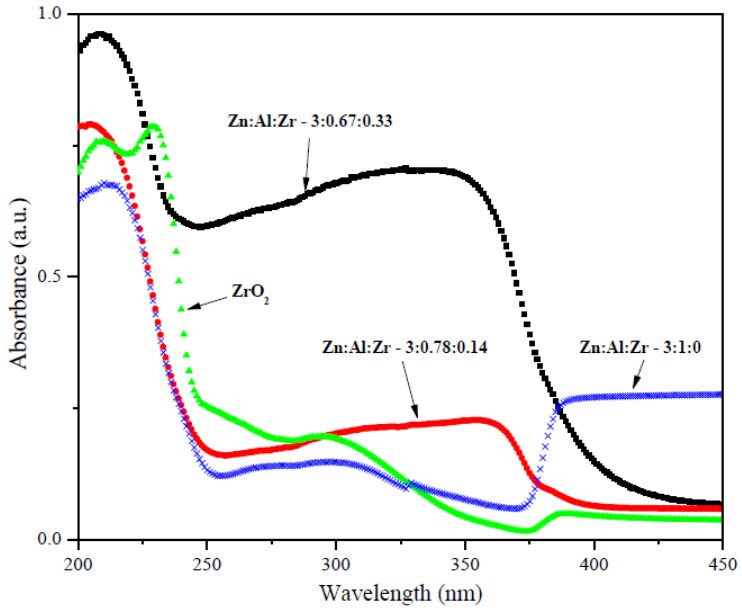

Figure S3. UV-VIS diffuse reflectance spectra of ZrO2 and ZnAlZr with different Zn:Al:Zr ratios.

At higher Zr4+ level, a chemical complexity may arise due to solid-solid phase separation [1] of a thin shell of ZrO2 from the LDH. To examine such a possibility and gain more information on the distribution of Zr4+ within the LDHs, UV-VIS DRS studies were carried out and the results are shown in Figure S3. All the LDH samples exhibited a single moderate band around 210 nm which is attributed to charge transfer involving isolated Zr4+ species [2, 3]. The absence of a pure ZrO2 band at 230 nm [4, 5] in all the LDHs samples, rules out the existence of significant amounts of ZrO2 within the LDHs. This is also supported by PXRD results which do not show the existence of a ZrO2 phase. The broad band with □max around 350 nm is due to O2 2-→Zr4+ ligand to metal charge transfer (LMCT) transitions.

Journal of Colloid and Interface Science, Vol. 363, No. 1 (August 2011): pg. 92-97. DOI.

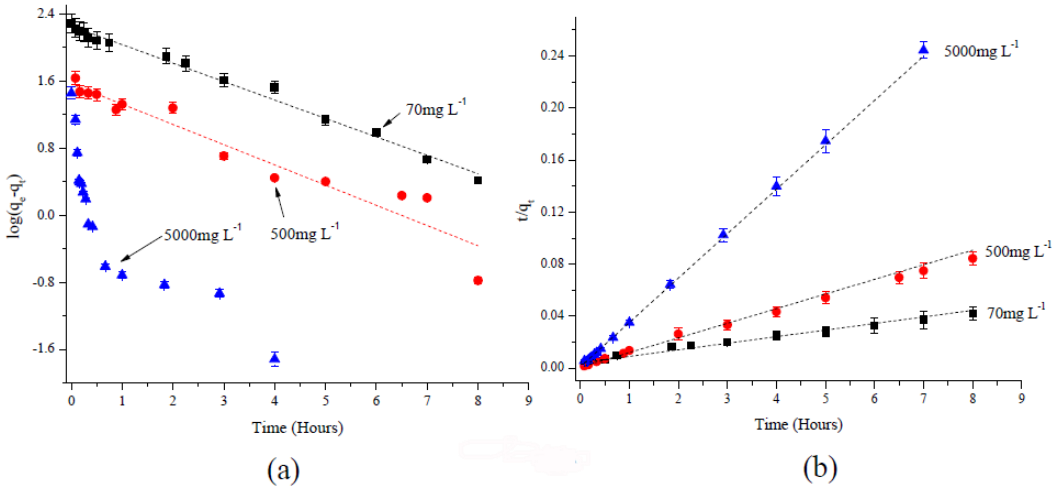

Figure S4. Adsorption kinetics models (a) pseudo-first order (b) pseudo-second order.

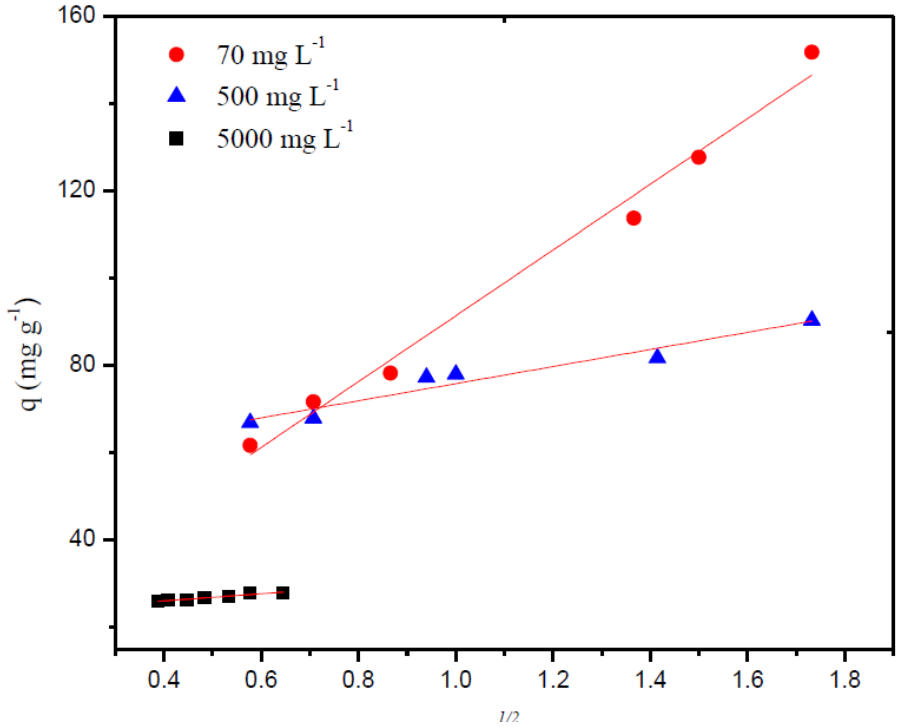

Figure S5. Intra-particle diffusion plots for adsorption of 2,4-D on ZnAlZr LDH for different adsorbent masses.

The calculated intra-particle diffusion constant, *kid*, values were 75.3±4.1, 19.6±2.4 and 8.2±0.9 mg g-1 h1/2 and intercept values

were 16, 56 and 22 for 70, 500 and 5000 mg L-1 adsorbent dosage, respectively. At low adsorbent dosage there is a greater contribution of the surface sorption in the rate limiting step as indicated by the larger intercept value. The contribution gets smaller when the adsorbent mass is increased. This, together with the fact that the intercept does not pass through the origin is an indicator that intra-particle diffusion is not solely rate controlling.

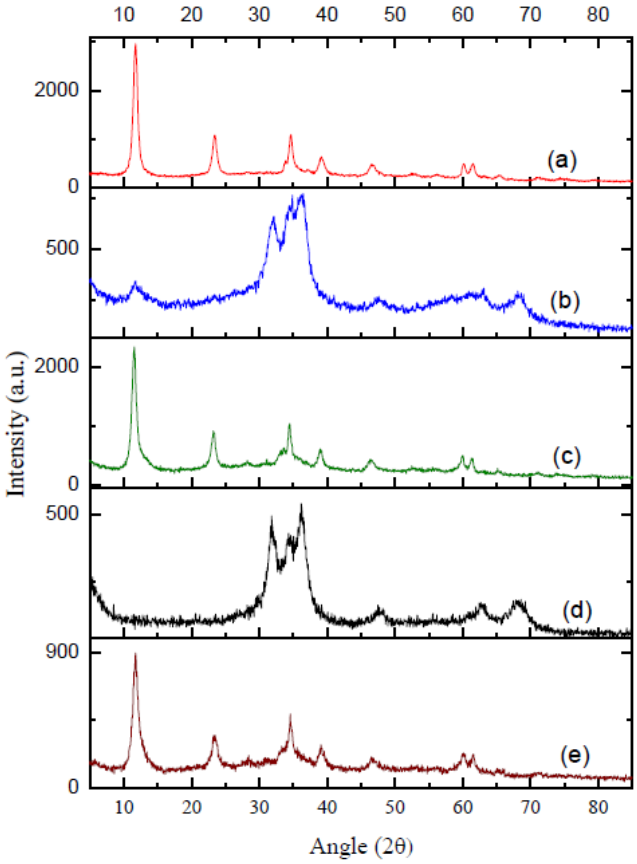

Figure S6. XRD diffractogram of ZnAlZr-LDH (a) as synthesized (b) and (d) Heated at 280oC after 2,4-D exposure, one and two cycles respectively. (c) and (e) Reconstituted in water after heating at 280oC, one and two cycles respectively.The phase at 280oC cannot be identified because the peaks are not well defined for indexing but is very likely a ZnO phase.

Finally, we note that no change is observed in the PXRD patterns after exposure of the LDHs to solutions containing 2,4-D. This indicates that adsorption, rather than anion exchange, is the dominant mode of uptake.

Journal of Colloid and Interface Science, Vol. 363, No. 1 (August 2011): pg. 92-97. DOI.

Table S1. Sample 1: ZnAl LDH without Zr, dried at 80oC.

	Calculated Formula (%)	Elemental Analysis Results (%)
Zn	46.717	45.76
Al	6.4216	6.29
H	2.4814	2.45
C	2.0112	1.97
O	42.349	43.53
Zr	0	0
∑	99.98	100

Sample 1 calculated Formula: Zn3Al(CO3)0.7(OH)7.61.4H2O

Table S2. Sample 2: ZnAlZr LDH dried at 80oC

	Calculated Formula (%)	Elemental Analysis Results (%)
Zn	46.084	46.25
Al	4.3144	4.33
H	2.2637	2.29
C	2.1622	2.17
O	40.585	40.37
Zr	4.5735	4.59
∑	99.982	100

Sample 2 calculated formula: Zn4.4AlZr0.3(CO3)1.1(OH)10.81.7H2O

Table S3. Sample 3 calcined at 80oC.

	Calculated Formula (%)	Elemental Analysis Results (%)
Zn	44.075	44.35
Al	6.092	6.13
H	2.238	2.27
C	1.4609	1.47
O	40.103	39.73
Zr	6.0125	6.05
∑	**99.982**	**100**

Sample 3 calculated formula: Zn3.0AlZr0.3(CO3)0.5(OH)9.1.0.4H2O

Journal of Colloid and Interface Science, Vol. 363, No. 1 (August 2011): pg. 92-97. DOI.

Table S4. Sample 4 calcined at 80oC.

	Calculated Formula (%)	Elemental Analysis Results (%)
Zn	43.312	43.68
Al	4.2538	4.29
H	2.2724	2.31
C	2.2013	2.22
O	40.892	40.39
Zr	7.0501	7.11
∑	**99.982**	**100**

Sample 4 calculated formula: Zn4.2AlZr0.5(CO3)1.2(OH)11.0.5H2O

Sample 2 calcined at 280oC with a molecular formula of Zn4.3AlZr0.3(CO3)0.3(OH)3.5O4.5 was used for all the adsorption experiments.

References for Supporting Information:

1. A. Chaparadza, S. B. Rananavare, V. Shutthanandan, *Mater. Chem. Phys.* **102** (2007), pp 176- 180.

2. B. Rakshe, V. Ramaswamy, A. V. Ramaswamy, *J. Catal.* **163** (1996), pp 501-505.

3. A. Tuel, S. Gontier, R. Teissier, *Chem.Commun.* (1996), pp 651-652.

4. D. Ciuparu, A. Ensuque, G. Shafeev, F. Bozon-Verduraz, *J. Mater. Sci. Lett.* **19** (2000), pp 931-933.

5. S. Velu, V. Ramaswamy, S. Sivasanker, *Chem. Commun.* (1997), pp 2107-2108.